Developing A Novel Dynamic Bus Lane Control Strategy With Eco-Driving Under Partially Connected Vehicle Environment

Xiaonian Shan[®], Changxin Wan, Peng Hao[®], Member, IEEE, Guoyuan Wu[®], Senior Member, IEEE, and Matthew J. Barth[®], Fellow, IEEE

Abstract-Exclusive bus lane strategy is widely adopted in many cities to improve bus operation efficiency and reliability. With the development of connected vehicle technologies, the dynamic bus lane (DBL) strategy was proposed, with allowing general vehicles to share use of the bus lane to improve traffic efficiency in general purpose lanes (GPLs). Previous studies have rarely considered the eco-driving strategy of connected and automated vehicles/buses (CAVs/CABs) in GPLs under the mixed traffic conditions, and how to ensure bus priority with DBL control. In this study, a novel DBL control strategy was developed under the partially connected vehicle environment. A trajectory planning method while considering the joint effects of bus stop and signal phase for CAB was adopted, an eco-driving strategy for CAVs in GPL was proposed using a trigonometry trajectory planning method. And a novel DBL control method was established by integrated trajectory planning for both the CAVs and CABs to ensure bus operation priority. Numerical experiments were conducted to evaluate performance of the proposed novel DBL control in terms of travel time and energy consumption of general vehicles at the different levels of CAV market penetration rates (MPRs). Results indicated that about 16%-42% energy savings can be achieved with MPR varying from 20% to 100%, and the travel time can be improved by about 4%-10%. Meanwhile, sensitivity analysis was conducted to quantify the impacts of key parameters, including vehicle target speeds, heterogeneous traffic flow, random arrival interval of cars, position of bus stop, traffic volume in GPLs and buffer length at the stop line of signalized intersections.

Index Terms—Dynamic bus lane control, connected and automated vehicle, trajectory planning, eco-driving, partially connected vehicle environment.

I. Introduction and Motivation

ROMOTING and improving bus service quality is considered as a highly effective way to mitigate urban traffic congestion and vehicle emissions by decreasing the usage of

Manuscript received 2 May 2023; revised 5 October 2023; accepted 16 November 2023. This work was supported in part by the National Natural Science Foundation of China under Grant 52002113; in part by the Natural Science Foundation of Jiangsu Province under Grant BK20200526; and in part by the Key Laboratory of Road and Traffic Engineering of the Ministry of Education, Tongji University under Grant K202302. The Associate Editor for this article was J. Hu. (Corresponding author: Xiaonian Shan.)

Xiaonian Shan and Changxin Wan are with the College of Civil and Transportation Engineering, Hohai University, Nanjing 210024, China (e-mail: shanxiaonian@hhu.edu.cn; changxin_wan@hhu.edu.cn).

Peng Hao, Guoyuan Wu, and Matthew J. Barth are with the Center for Environmental Research and Technology, University of California at Riverside, Riverside, CA 92507 USA (e-mail: haop@cert.ucr.edu; gywu@cert.ucr.edu; barth@ece.ucr.edu).

Digital Object Identifier 10.1109/TITS.2023.3336895

private-owned cars. The strategy of exclusive bus lanes has been adopted widely in many cities to improve bus operation efficiency and service quality [1]. For example, there were about 223 km of bus lanes in New York City in 2021. Due to the effects of bus lane configurations, signalized intersections, and interruption of general traffic, the improvement in bus operation is not satisfactory [2]. Specifically, a single curbside bus lane is rarely effective because of the impact of bicyclists and right-turning vehicles [3], and signalized intersections can also result in much more bus delays due to the lack of bus signal priority system [4]. Moreover, designs of exclusive bus lanes often require a substantial allocation of road space, potentially exacerbating for general traffic during peak hours.

Recently, with the development of information and communication technology, collaborative intelligence for internet of vehicles can be achieved under the cooperative vehicle infrastructure system. Connected and Automated Buses (CABs) are becoming a reality in some pilot demonstration projects to improve bus operational efficiency and ensure bus safety at all times [5]. Trajectory planning methods for CABs driving in bus lanes were proposed by leveraging the Signal Phase and Timing (SPaT) messages broadcast from Roadside Units (RSUs). Shan et al. proposed a bi-level programming model to realize the Eco-Approach and Departure (EAD) system of CABs at signalized intersections with bus stops [6]. In a mixed traffic flow where Connected and Automated Vehicles (CAVs) and Human-driven Vehicles (HDVs) co-exist in general purpose lanes, CAVs can receive the related SPaT information to adjust their traveling speeds using eco-driving strategies [7]. Furthermore, in the context of bus priority, CAVs could be allowed to use the available time-space span in the bus lane to mitigate traffic congestion in general purpose lanes, which can improve the road utilization of bus lanes. Therefore, a novel dynamic bus lane control strategy is proposed and evaluated under partially connected vehicle environment in this study.

In the literature, various studies have explored the operational performance and influential factors of dedicated bus lanes. Shalaby analyzed the bus delays and auto speeds using the TRANSYT-7F simulator [8]. The results showed that while the average bus speed improved after the introduction of bus lanes, the performance of adjacent traffic deteriorated. However, the bus travel times showed longer than the adjacent general traffic due to the increase in bus dwell times at stops. Farid et al. proposed an analytical model to evaluate the impact

1558-0016 © 2024 IEEE. Personal use is permitted, but republication/redistribution requires IEEE permission. See https://www.ieee.org/publications/rights/index.html for more information.

of nearside bus stops on auto and transit vehicle delays. Bus personal delay was decreased by more than 50 percent in dedicated bus and queue jumper lanes compared with normal conditions [9]. Shen et al. developed analytical approximations for the bus capacity at near- and far-side bus stops in a dedicated bus lane, considering the effect of signal timings and distances between bus stops and signals [10]. Cui et al. proposed a novel multivariate conditional autoregressive model to explore the contributing factors to bus traveling speed, such as number of lanes, with or without dedicated bus lanes, bus stop location, signal timing and so on [11].

On the other hand, the intermittent bus lane (IBL) was proposed to improve bus lane utilization and mitigate general traffic congestion. For a road segment, when a bus enters the IBL, downstream vehicles should exit the lane, except for right-turning vehicles, to prioritize bus operation [12]. Yang and Wang then proposed a Dynamic Bus Lane (DBL) system under certain traffic situations to allocate roadway resources in a productive manner [13]. When a bus is detected, the downstream curbside lane between two adjacent signalized intersections is restricted for buses. Compared with IBL, vehicles ahead of the bus can be allowed driving in the exclusive bus lane. Recently, with the development of vehicle-to-vehicle communications, Wu et al. developed the bus lanes with intermittent and dynamic priority to address the limitations of traditional IBL. Upstream vehicle drivers can be alerted when a bus is in the lane [14]. Szarata and Olszewski [15] proposed a new model for DBL control, then calibrated and validated the control model in the PTV Vissim traffic simulation software. Results indicated that their proposed DBL control model improves the average travel time for private transport while maintaining travel time savings for buses. A Similar methodology was also adopted by Kampouri et al [16]. Xie et al. proposed a flexible bus priority lane system that utilized connected vehicles technology, analyzing the impacts of penetration rate and communication range of CAVs using a microscopic simulation approach. Results revealed that buses could benefit significantly in a communication range of 150 m [17]. Luo et al. developed a dynamic bus lane with moving block in a connected-vehicle environment using cellular automata model [18]. Yang and Oguchi developed an optimal dynamic path planning system to improve vehicle mobility with consideration of bus stops [19]. Othman et al. [20] analyzed the total person delay of DBL control strategy in comparison to the exclusive bus lane and mixed lane (without bus priority) control strategy under different traffic demand and bus service frequency. The simulated experiments were conducted by Aimsun Next as a case study of the Eglinton East corridor in Toronto, Canada, and all cars are assumed as connected vehicles. The results revealed that the DBL control strategy outperforms the other control strategies over a wide range of traffic demand and transit service conditions, especially under the intermediate traffic demand levels.

Previous studies have demonstrated that the location of bus stops and signalized intersections significantly affects the performance of dedicated bus lanes. To address the limitations of IBL, strategies of DBL have been proposed using connected vehicle technology, mainly focused on the control methods of general vehicles. However, under the cooperative vehicle infrastructure system, the trajectory of CAB can be planned while considering the combined effects of bus stops and signalized intersections to reduce bus energy consumption. Meanwhile, the EAD control method of CAVs driving in general purpose lane can be adopted to achieve the efficiency and energy benefits. CAVs are permitted to lane change into the dedicated bus lane to increase the bus lane utilization and improve the general traffic, as shown in Figure 1. The trajectory planning algorithm of CAVs should be proposed without conflicting with the trajectory of CAB to ensure the bus priority.

In response to the concerns of traditional IBL and shortcomings of previous DBL strategies, the objective of this study is to propose a novel dynamic bus lane control strategy with eco-driving under partially connected vehicle environment. More specially, the trajectory planning methods of CABs and CAVs in dynamic bus lanes should be proposed while considering the impacts of bus stops and signal timings. An eco-driving method will be applied to CAVs in general purpose lanes, and a DBL control strategy will be proposed to optimize the utilization of bus lanes. The main contributions of this study are summarized as follows: (1) Proposing an eco-driving strategy for CAVs in general purpose lane under partially connected vehicle environment. (2) Designing an eco-driving strategy for CAENs while considering the joint effect of bus stop and signalized intersection. (3) Developing a novel DBL strategy that accounts for the eco-driving strategies of CAVs and CAEB. (4) Analyzing the benefits of the novel DBL strategy with different road and traffic flow parameters.

The remainder of this paper is organized as follows. The methodology of the novel DBL control strategy is proposed in Section II. Section III conducts the numerical experiments under different levels of CAV Market Penetration Rate (MPR). Section IV shows the results of sensitivity analyses with seven different influencing factors. The paper ends up with conclusions and discussion of future steps in Section V.

II. METHODOLOGY

In this section, the novel DBL control strategy with eco-driving under partially connected vehicle environment is proposed. We first describe the proposed problem, and point out the basic model assumptions. Energy consumption models for buses and cars are presented. Then the trajectory planning method for the Connect and Automated Electric Bus (CAEB) is introduced while considering the joint effect of bus stops and signalized intersections. Human driver model is also presented, and the eco-driving strategy for CAVs in general purpose lane is proposed. Finally, the novel dynamic bus lane control strategy is proposed, allowing CAVs driving into the bus lane on the premise of ensuring bus priority.

A. Problem Description

As illustrated in Figure 1, we consider a signalized roadway intersection with some roadside units (RSUs) under partially CAV environment in this study. There exist two types of road lanes, i.e., GPL for HDVs and CAVs, and DBL for

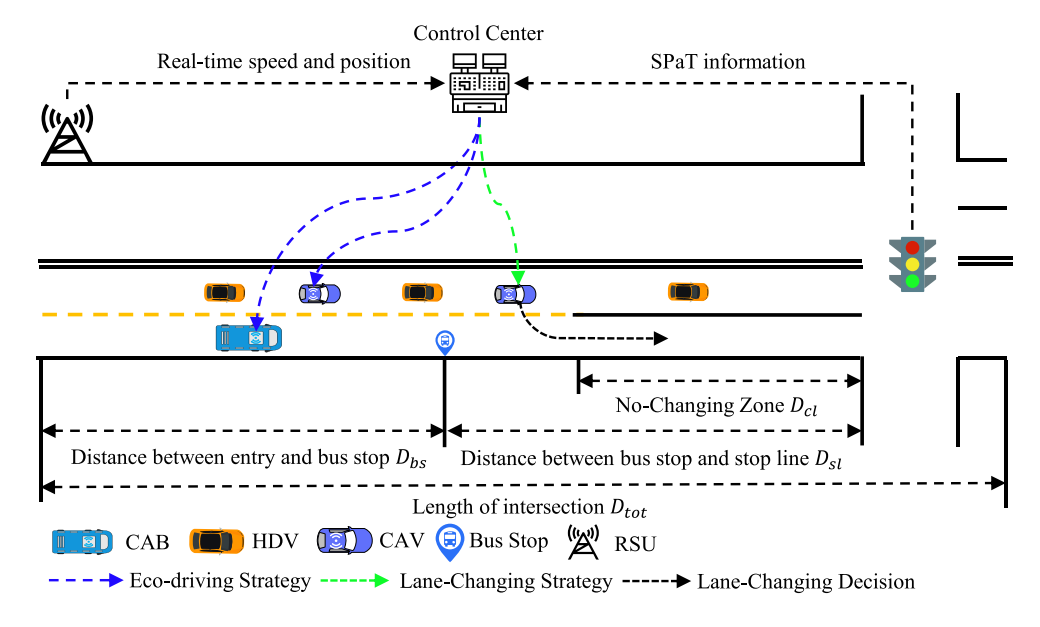


Fig. 1. The proposed novel dynamic bus lane control method.

CABs. It is also assumed that some CAVs can drive into the bus lane through lane changing behaviors under certain conditions. There is a buffer zone close to the stop line of the intersection, where lane changing is prohibited. All the CABs and CAVs can receive the SPaT information from signalized intersections and vehicle driving states, i.e., vehicle speed, location and acceleration, in the communication distance. Thus, the trajectories of CAB and CAVs can be optimized using such information with the objective of reducing energy consumption and improving road utilization efficiency of bus lane.

To enhance eco-driving for CABs in DBL, it is crucial to consider the joint effect of bus stops and signalized intersections. Typically, the bus stop is located upstream of the intersection, the process of driving through the signalized intersection can be divided into three parts: driving to the bus stop, dwelling at the bus stop, and passing through the intersection. To optimize the energy consumption, it is essential to estimate both travel time and energy usage for each of these parts. In the context of eco-driving for in GBL, the ego CAV can utilize the SPaT information to pass through the intersection without stopping, which can further reduce energy consumption. However, CAVs must also fine-tune their speed profiles to maintain a safe distance from each other.

In the implementation of the DBL control strategy, CAVs should consider lane changing behaviors to use the DBL effectively without compromising bus operations. While the basic motivation of lane changes is often to achieve higher speeds, it is essential to prioritize avoiding conflicts between CAV and planned CAB trajectories. In other words, CAVs should be able to drive into the DBL without interfering with the bus lane. See Figure 1 for a visual representation of this strategy.

B. Energy Consumption Models for Buses and Vehicles

Traditional diesel buses had been widely replaced by electric buses to reduce emissions and energy consumption. In this study, we assume that the bus driving in the bus lane is a battery electric bus, and other vehicles are all gasoline cars.

1) Gasoline Vehicle Energy Consumption Model: For the gasoline cars (HDVs and CAVs), the power-based energy consumption model developed by Biggs and Akcelik is adopted in this study [21], as follows:

$$g(v, a; t) = \bar{\alpha} + \begin{cases} \max\left\{\beta_1 v R(v, a) + \beta_2 m v a^2, 0\right\}, & if \ a \ge 0 \\ \max\left\{\beta_1 v R(v, a), 0\right\}, & otherwise \end{cases}$$
(1)

where v and a are car speed and acceleration, respectively. m is the mass of an average passenger car. $\bar{\alpha}$ is the idling gasoline consumption rate. β_1 is the parameter relevant to the energy efficiency of the engine, and β_2 is the gasoline consumption parameter when a is greater than zero. R(v, a) is the total tractive force required to drive the car and satisfies the following equation:

$$R(v, a) = b_1 + b_2 v^2 + ma + mg \sin \theta$$
 (2)

where b_1 , b_2 are the parameters related to car rolling resistance and aerodynamic drag. g represents the gravitational acceleration. θ represents the road grade (positive for uphill and negative for downhill).

Based on Equation (1) and Equation (2), the eco-cruising speed of a general vehicle (v_{eco}) that represents the speed related to minimal energy consumption per mile can be obtained using the following equation (3). More details could be found in literature [22].

$$v_{eco} = arg \min_{0 \le v \le v_{v,\text{max}}} \frac{\int g(v, 0; t)dt}{\int vdt} = \sqrt[3]{\frac{\bar{\alpha}}{2\beta_1 b_2}}$$
(3)

2) Electric Bus Energy Consumption Model: Several power consumption models are available for electric buses, including power-based model and data-driven based model. In this study,

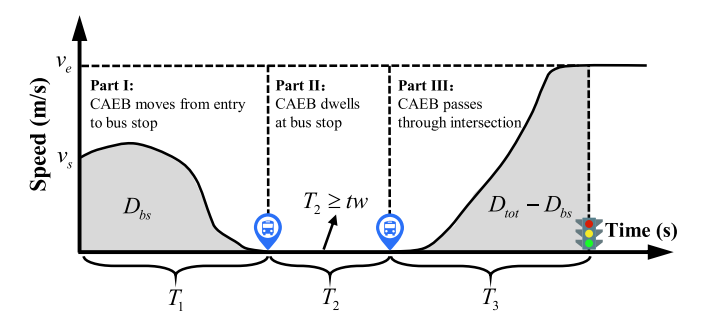


Fig. 2. Operation modes of a bus passing through the intersection.

the powertrain-based model is used to estimate electric bus energy consumption [23], as follows:

$$p(v, a; t) = \begin{cases} \tau(v, a) \cdot \omega(v) \cdot \tilde{\eta}(\tau, \omega), & \text{if } F(v, a) \ge 0\\ -\eta_{wh} \eta_{fd} \eta_{mot} \eta_{batt} \tau(v, a) v, & \text{otherwise} \end{cases}$$
(4)

where $\tau(v,a)$ is the bus motor torque; $\omega(v)$ is the motor speed. $\tilde{\eta}(\tau,\omega)$ is the efficiency map derived from Riverside Transit Agency (RTA). F(v,a) is the bus traction force, η_{wh} , η_{fd} , η_{mot} , η_{batt} are the related parameters of driveline efficiency, final drive efficiency, electric motor efficiency, and battery efficiency. $\tau(v,a)$, $\omega(v)$ and F(v,a) are calculated using the following equations:

$$\tau(v,a) = F(v,a)/\eta s \tag{5}$$

$$\omega(v) = sv \tag{6}$$

$$F(v, a) = Ma + f_{rl}Mg\cos\theta + Mg\sin\theta + kv^2$$
 (7)

where η is the overall powertrain efficiency. s is the gear ratio determined by the gear level. M represents the mass of a normal bus. f_{rl} , and k represent the bus rolling and aerodynamic resistance coefficient. θ represents the road grade (positive for uphill and negative for downhill).

A conversion coefficient ρ_c is used to convert fuel consumption of cars with the unit of milliliter (mL) into the unit of kilojoule (kJ). The value of the conversion coefficient is 31.25, derived from China Energy Statistical Yearbook 2022.

C. Trajectory Planning for CAEB in Dedicated Bus Lane

As illustrated in Figure 2, the trajectory for buses can be divided into three parts: 1) gliding to the vicinity of the bus stop and decelerating to zero speed; 2) dwelling at the bus stop; and 3) accelerating to pass through the signalized intersection with the assumption of no other traffic interruption. D_{tot} is the total distance for the road section, and D_{bs} is the distance of the first part. v_s and v_e represent the initial and terminal speed of buses. A bi-level programming model was proposed in our previous research [6] to obtain the optimal trajectories of CAEBs in exclusive bus lane, which is adopted in this study. For each part i, the bus initial states, including position $x_{s,i}$, speed $v_{s,i}$, and time $t_{s,i}$, denoted by a vector $(x_{s,i}, v_{s,i}, t_{s,i})$, and the terminal state $(x_{e,i}, v_{e,i}, t_{e,i})$ is determined. The lower-level problem is thus to solve three optimal control problems (one for each part) with given initial and terminal conditions.

1) Lower-Level Problem: The mathematical formulation of the lower-level problem for each part of bus trajectory planning is presented in Equations (8)-(14).

$$MinE_i = \int_{t_{s,i}}^{t_{e,i}} p(v, a; t) dt, \quad \forall i = 1, 2, 3$$
 (8)

Subject to:
$$\dot{x}(t) = v(t)$$
, and $\dot{v}(t) = a(t)$ (9)

$$0 \le v(t) \le v_{b,\text{max}} \tag{10}$$

$$a_{b,\min} \le a(t) \le a_{b,\max}$$
 (11)

$$t_{s,i} \le t \le t_{e,i}, \quad \forall i = 1, 2, 3$$
 (12)

$$v(t_{s,i}) = v_{s,i}, and x(t_{s,i}) = x_{s,i}, \quad \forall i = 1, 2, 3$$

(13)

$$v(t_{e,i}) = v_{e,i}, and x(t_{e,i}) = x_{e,i}, \quad \forall i = 1, 2, 3$$
(14)

where Equation (8) aims to minimize the energy consumption of the bus trajectory in part i. Equation (9) describes the relationship among the bus position, velocity, and acceleration. Equation (10) requires that the bus speed must be higher than zero, and cannot exceed the maximum speed $(v_{b,\text{max}})$. Equation (11) states that the acceleration should be within the range between the minimum $(a_{b,\text{min}})$ and maximum $(a_{b,\text{max}})$ acceleration. Equation (12) represents the range of driving time. Equation (13) and Equation (14) constrain the initial and terminal state conditions.

A graph model is used to solve the lower-level problem, where the time and space are discretized into fixed time t_{Δ} (1 s) and distance grid d_{Δ} (1 m). In that case, the lower problem is equal to searching the shortest energy consumption path from the initial state $(x_{s,i}, v_{s,i}, t_{s,i})$ to the terminal state $(x_{e,i}, v_{e,i}, t_{e,i})$, which can be solved by Dijkstra algorithm.

2) Upper-Level Problem: The upper-level program represents the travel time assignment for the three parts in Figure 2, i.e., the time driving to the bus stop (T_1) , the time stopping at the bus stop (T_2) , and the time driving to the downstream intersection (T_3) . The objective of this problem is to obtain the least energy consumption of bus trajectory with a suitable travel time. The decision variables in the upper-level program have impacts on the lower problem with the variational time. For each scenario with $T = [T_1, T_2, T_3]$, the formulation to minimize the objective is as follows:

$$Min \sum E_i + cc \times \sum T_i \tag{15}$$

Subject to:
$$t_{e,i} - t_{s,i} = T_i$$
, $\forall i = 1, 2, 3$ (16)

$$t_{e,i} - t_{s,i+1} = 0, \quad \forall i = 1, 2$$
 (17)

$$0 \le T_i \le t_{cyc}, \quad \forall i = 1, 2, 3$$
 (18)

$$T_2 > tw \tag{19}$$

$$\left(\left\lceil \frac{t_{sl}}{t_{cyc}}\right\rceil - 1\right)t_{cyc} \le t_{sl} \le \left\lceil \frac{t_{sl}}{t_{cyc}}\right\rceil t_{cyc} - t_{red}$$
 (20)

Subject to:
$$E_i = Min \int_{t_{s,i}}^{t_{e,i}} p(v, a; t) dt$$
, $\forall i = 1, 2, 3$

(21)

where E_i , T_i represent the energy consumption and travel time in part i. cc is the equivalent factor for the balance of

bus energy consumption and traveling time. tw presents the bus dwelling time at bus stop. t_{cyc} is the cycle length of the intersection. t_{red} is the length of red time. and t_{sl} is the time instant when the bus is located at the stop line.

The upper-level problem is an integer programming with finite solution set. Therefore, implicit enumeration method is selected to solve the upper problem. For each CAEB, its trajectory is determined at its entry time by the bi-level programming model.

D. Human Driver Model in General Purpose Lane

In this study, a revised Intelligent Driver Model (IDM) [24] is selected to generate and update the acceleration of HDVs, which is widely used to simulate the trajectories of HDV. Vehicle acceleration values calculated by IDM can be divided into two orders: (1) the accelerate order, and (2) the brake order. The accelerate order is limited by the current car itself can be calculated as follows:

$$a_n^f(t) = a_{c,\text{max}} \left[1 - \left(\frac{v_n(t)}{v_n^d} \right)^4 \right]$$
 (23)

where $a_{c,\text{max}}$ is the maximum acceleration of a certain HDV. $v_n(t)$ is the velocity of the *n*-th HDV at time *t*. and v_n^d is the desired velocity of the *n*-th HDV, which is equal to car's maximum speed $v_{c,\text{max}}$.

The brake order is determined by two factors: the velocity difference between the ego vehicle and its preceding car, represented by $(\Delta v_n(t))$, and the space error between them, represented by $(\Delta x_n(t))$. These values are calculated using Equations (24) and (25).

$$\Delta v_n(t) = v_n(t) - v_{n,p}(t) \tag{24}$$

$$\Delta x_n(t) = x_{n,p}(t) - x_n(t) - l_{n,p}$$
 (25)

where $v_{n,p}(t)$ and $x_{n,p}(t)$ represent velocity and position of the preceding vehicle at time t, and $l_{n,p}$ denotes the length of preceding vehicle.

Then the acceleration of brake order that represents the impact of preceding vehicle $a_n^c(t)$ can be calculated by Equation (26), as follows:

$$a_n^c(t) = -a_{c,\max} \left[\frac{s_0 + \tau v_n(t) + v_n(t) \Delta v_n(t) / \sqrt{|a_{c,\max} a_{c,d}|}}{\Delta x_n(t)} \right]^2$$
(26)

where s_0 is the jam gap. τ is the safe time headway of two consecutive vehicle. and $a_{c,d}$ is the comfortable deceleration.

The final acceleration $a_n^v(t)$ is the sum of the above accelerations, which is a function of the current speed, related speed, and space error:

$$a_n^v(t) = a_n^f(t) + a_n^c(t) = f(v_n(t), \Delta v_n(t), \Delta x_n(t))$$
 (27)

Figure 3 depicts the trajectory generation scheme for one HDV at each time step Δt . The HDV will maintain the acceleration $a_n^v(t)$ if the vehicle can pass the signalized

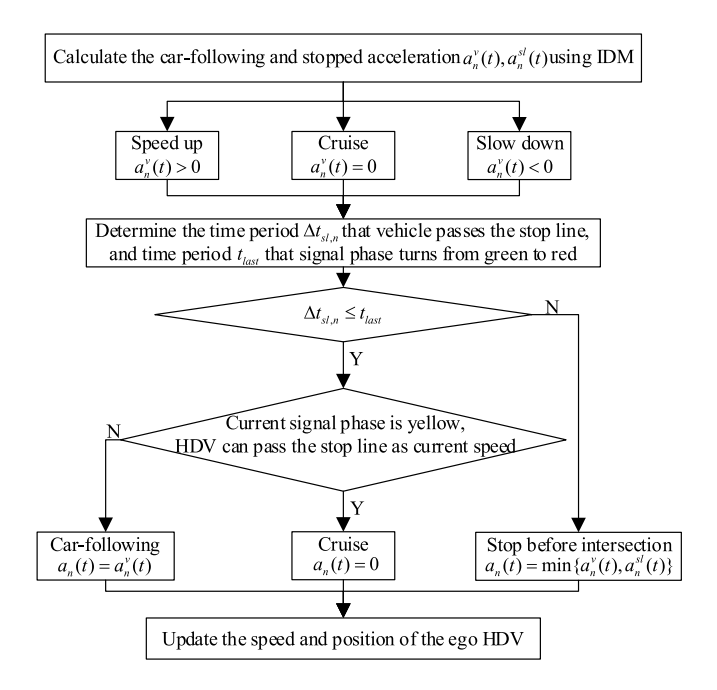


Fig. 3. The control scheme of HDVs' driving behavior.

intersection during the green or yellow phase. If the HDV cannot pass the intersection or the current signal phase is red, it will idle before the stop line. Thus, three acceleration values are identified during the driving process of the HDV: $(1) a_n^v(t) > 0$; $(2) a_n^v(t) = 0$; and $(3) a_n^v(t) < 0$.

When $a_n^v(t)$ is greater than zero, the HDV can pass the stop line, the time period $\Delta t_{sl,n}$ that HDV drives from current position to stop line is calculated as follows:

$$\Delta t_{sl,n} = \begin{cases} \frac{-v_n(t) + \sqrt{v_n^2(t) + 2a_n^v(t) \times (x_{sl} - x_n(t))}}{a_n^v(t)}, & t_{a,n} \ge t_{last} \\ t_{a,n} + \frac{2(x_{sl} - x_n(t)) - t_{a,n} \times (v_n(t) + v_n^d)}{2v_{c,\max}}, & t_{a,n} < t_{last} \end{cases}$$
(28)

where x_{sl} is the position of stop line, $t_{a,n}$ is the acceleration time from current speed $(v_n(t))$ to the limit speed $(v_{c,max})$ using Equation (29). t_{last} is time period that signal phase turns from green to red, using Equation (30).

$$t_{a,n} = \left(v_{c,max} - v(t)\right) / a_n^v(t) \tag{29}$$

$$t_{last} = \max\left\{0, \left\lceil \frac{t}{t_{cyc}} \right\rceil t_{cyc} - t - t_{red} \right\}$$
 (30)

When $a_n^v(t)$ is equal to zero, $\Delta t_{sl,n}$ can be calculated using Equation (31).

$$\Delta t_{sl,n} = t_{cs,n} = (x_{sl} - x_n(t))/v_n(t)$$
 (31)

where $t_{CS,n}$ represents the time period that HDV drives from current position to stop line as a velocity of $v_n(t)$.

When $a_n^v(t)$ is less than zero, $\Delta t_{sl,n}$ can be calculated as follows:

$$\Delta t_{sl,n} = \begin{cases} \frac{-v_n(t) + \sqrt{v_n^2(t) + 2a_n^v(t) \times (x_{sl} - x_n(t))}}{a_n^v(t)}, \\ t_{d,n} \ge t_{last} \\ \infty, \quad t_{d,n} < t_{last} \end{cases}$$
(32)

where $t_{d,n}$ is the deceleration time from current speed $(v_n(t))$ to zero, which is calculated by $-v_n(t)/a_n^v(t)$.

The acceleration of $a_n^{sl}(t)$ denotes the acceleration of the HDV considering the impact of stop line, using the following equation.

$$a_n^{sl}(t) = f(v_n(t), -v_n(t), x_{sl} - x_n(t))$$
(33)

where $f(v_n(t), -v_n(t), x_{sl} - x_n(t))$ is the function of IDM. $-v_n(t)$ is related to speed $\Delta v_n(t)$, and $x_{sl} - x_n(t)$ represents the space error $\Delta x_n(t)$.

If $\Delta t_{sl,n} \leq t_{last}$, i.e., the HDV can pass the stop line before red phase, it will maintain the acceleration $a_n^v(t)$. If $\Delta t_{sl,n} > t_{last}$, the HDV should stop before the stop line, the acceleration of the HDV must be neither lower than car-following acceleration $a_n^v(t)$ nor stop line acceleration $a_n^{sl}(t)$. Particularly, if the current signal phase is yellow, the HDV can pass the intersection as the current speed $v_n(t)$, the acceleration of such HDV will be zero while considering safety. Thus, the acceleration of HDV can be determined as follows:

$$a_{n}(t) = \begin{cases} 0, & \text{if } t_{cs,n} \leq t_{last}, 0 \leq t_{last} - t_{gre} < t_{yel} \\ \min\{a_{n}^{v}(t), a_{n}^{sl}(t)\}, & \text{if } \Delta t_{sl,n} > t_{last} \\ a_{n}^{v}(t), & \text{otherwise} \end{cases}$$

$$(34)$$

The position and speed of the HDV at next step $(t + \Delta t)$ can be updated as follows:

$$v_n(t + \Delta t) = v_n(t) + a_n(t)\Delta t \tag{35}$$

$$x_n(t + \Delta t) = x_n(t) + \frac{v_n(t) + v_n(t + \Delta t)}{2} \Delta t$$
 (36)

Thus, we can obtain the trajectories of HDVs.

E. Eco-Driving for CAVs in General Purpose Lane

As stated in the previous section, if $\Delta t_{sl,n} > t_{last}$, the HDV will stop before the stop line of GPL. By utilizing real-time SPaT information along with data on the preceding vehicles, CAVs may establish an eco-driving method that enables them to pass through intersection without the need to stop. The proposed method is presented as below:

I) Travel Time Estimation for CAVs: A scheme of travel time estimation is illustrated in Figure 4. Firstly, it is assumed that there is no vehicle in front of the ego CAV. If $\Delta t_{sl,n} \leq t_{last}$, the CAV can pass through the intersection without any stops. Thus, there is no need for taking eco-driving method. If $\Delta t_{sl,n} > t_{last}$, the CAV can pass through the signalized intersection at the next green phase, we assume that the CAV

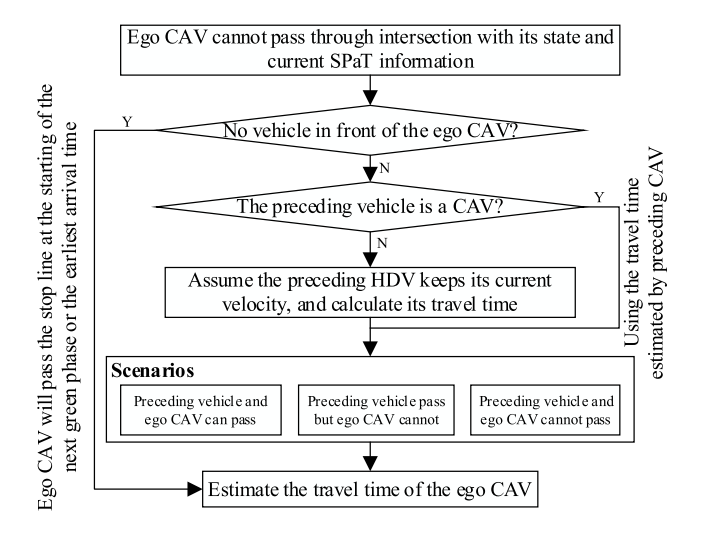


Fig. 4. The scheme of travel time estimation for CAVs.

can pass the stop line at the earliest arrival time or at the starting of the next green phase, thus we can get

$$= \max \left\{ \left\lceil \frac{t}{t_{cyc}} \right\rceil t_{cyc}, t + \frac{x_{sl} - x_n(t)}{v_{c,\text{max}}} + \frac{\left(v_{c,\text{max}} - v_n(t)\right)^2}{2v_{c,\text{max}}a_{c,\text{max}}} \right\}.$$

If there exist vehicles in front of the ego CAV, $t_{sl,n}$ is determined by its preceding vehicles and SPaT information. We set the vehicle position and speed in front of this CAV is $x_{n,p}(t)$ and $v_{n,p}(t)$, respectively. If the preceding vehicle is an HDV, we assume that its speed keeps as constant, so the time $(t_{sl,n}^p)$ that the preceding vehicle passing through the stop line can be determined. If the preceding vehicle is a CAV, the current CAV can obtain the passing time of the preceding CAV directly. Thus, $t_{sl,n}^p$ can be estimated as follows:

$$t_{sl,n}^{p} = \begin{cases} t_{sl,n}^{p}, & \text{if the preceding vehicle is CAV} \\ t + \frac{x_{sl} - x_{n,p}(t)}{v_{n,p}(t)}, & \text{otherwise} \end{cases}$$
(37)

With the consideration of the current SPaT information and $t_{sl,n}^p$, $t_{sl,n}$ can be calculated as follows:

$$t_{sl,n} = \begin{cases} t_{sl,n}^{p} + t_{hw}, t_{sl,n}^{p} \in \left[\left(\left\lceil \frac{t}{t_{cyc}} \right\rceil - 1 \right) t_{cyc}, t_{r} - t_{hw} \right] \cup \\ \left[\left\lceil \frac{t}{t_{cyc}} \right\rceil t_{cyc}, t_{r}' - t_{hw} \right] \end{cases}$$

$$= \begin{cases} \frac{t}{t_{cyc}} \left\lceil t_{cyc}, t_{sl,n}' \right\rceil \in \left[t_{r} - t_{hw}, t_{r} \right] \cup \left[t_{r}' - t_{hw}, t_{r}' \right] \\ \left\lceil \frac{t}{t_{cyc}} \right\rceil t_{cyc} + t_{ls} + N_{p} t_{hw}, t_{sl,n}^{p} \in \left[t_{r}, \left\lceil \frac{t}{t_{cyc}} \right\rceil t_{cyc} \right] \\ \cup \left[t_{r}', \infty \right] \end{cases}$$
(38)

$$t_r = \left(\left\lceil \frac{t}{t_{cyc}} \right\rceil - 1 \right) t_{cyc} + t_{gre} + t_{yel}$$
 (39)

$$t_r' = \left\lceil \frac{t}{t_{cyc}} \right\rceil t_{cyc} + t_{gre} + t_{yel} \tag{40}$$

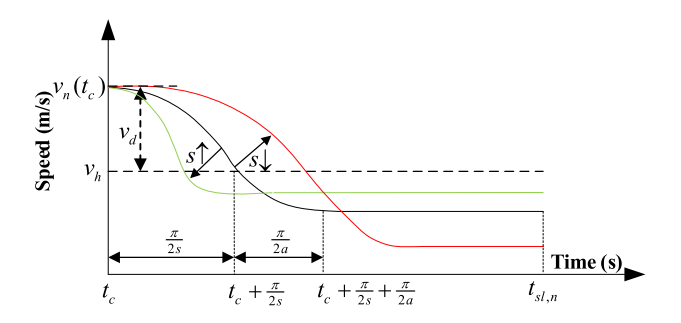


Fig. 5. The speed profile of trigonometry method.

where t_{hw} is the saturation time headway, which equals to the reciprocal of maximal volume determined based on the fundamental diagram of IDM. t_r is the time with current signal phase turning to red, which can be calculated using the Equation (39). t'_r is the time with the next signal phase turning to red. t_{ls} is the start time at the beginning of green phase, and N_p is the number of preceding vehicles with respect to current CAV before the stop line.

The first branch in Equation (38) represents the case that the ego and preceding vehicle can pass through stop line before red phase, $t_{sl,n}$ is set as $t_{sl,n}^p + t_{hw}$ to ensure vehicle travel efficiency. The second branch represents the case that the preceding vehicle can pass through stop line before red phase, while the current CAV cannot pass through the stop line in time, $t_{sl,n}$ is equal to $\left\lceil \frac{t}{t_{cyc}} \right\rceil t_{cyc}$. The last branch represents the case the preceding vehicle cannot pass through stop line before red phase, and there are N_p number of vehicles in front of the preceding vehicle, where $t_{sl,n}^p$ is set to $\left\lceil \frac{t}{t_{cyc}} \right\rceil t_{cyc} + t_{ls} + (N_p - 1) \times t_{hw}$ and $t_{sl,n}$ is set to $t_{sl,n}^p + t_{hw}$.

2) Trigonometry Method for CAV Trajectory Planning: The trigonometry method is proposed for CAV trajectory planning while considering the computational efficiency. The speed profile of trigonometry method is illustrated in Figure 5. For given values of $t_{sl,n}$ and t_c (the current time), the speed curve at time period t ($t \in [t_c, t_{sl,n}]$) of the CAV could be described as follows [25]:

$$v_{n}(t) = \begin{cases} v_{h} + v_{d}\cos(st), & t \in \left[t_{c}, t_{c} + \frac{\pi}{2s}\right) \\ v_{h} + \frac{s}{a}v_{d}\cos a(t - \frac{\pi}{2s} + \frac{\pi}{2a}), \\ & t \in \left[t_{c} + \frac{\pi}{2s}, \quad t_{c} + \frac{\pi}{2s} + \frac{\pi}{2a}\right) \\ v_{h} + \frac{s}{a}v_{d}, & t \in \left[t_{c} + \frac{\pi}{2s} + \frac{\pi}{2a}, t_{sl,n}\right) \end{cases}$$

$$(41)$$

where v_h is the average speed at time period t, calculated by $v_h = \min\left\{v_{c,\max}, \frac{x_{sl} - x_n(t_c)}{t_{sl,n} - t_c}\right\}$. v_d is the speed difference between the current speed $v_n(t_c)$ and the average speed v_h , calculated by $v_d = v_n(t_c) - v_h$. (s, a) control the rate of change of acceleration, different values of (s, a) show the different acceleration and jerk profiles.

Based on previous research [25], to minimize energy consumption, parameter *s* should be chosen as large as possible, with the spatio-temporal, vehicle acceleration and jerk

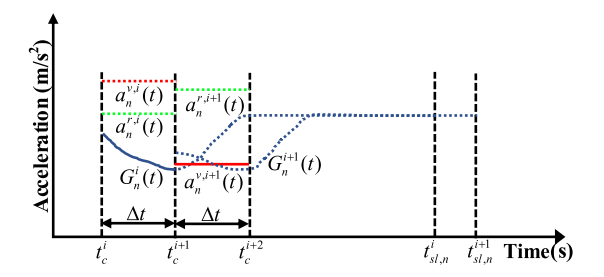


Fig. 6. Rolling horizon scheme for CAV's eco-driving strategy.

constraints, s is determined as follows:

$$\max_{s \in \{0,1\}} \{s\} \tag{42}$$

Subject to:
$$\int_{t_{c}}^{t_{sl,n}} v_{n}(t)dt = x_{sl} - x_{n}(t_{c})$$

$$a_{c,\min} \leq \frac{v_{d}}{|v_{d}|} \cdot \left[\max_{t \in [t_{c}, t_{sl,n}]} \{|a_{n}(t)|\} = |v_{d}s| \right]$$

$$\leq a_{c,\max}$$

$$\max_{t \in [t_{c}, t_{sl,n}]} \{|jerk_{n}(t)|\} = |v_{d}sa| \leq k_{\max}$$
(45)

where $jerk_n(t)$ represents the rate of change of acceleration at time t, and k_{max} represents the maximal jerk.

Equation (43) states that the CAV passes the stop line at time of $t_{sl,n}$. Equation (44) and Equation (45) show the range of acceleration and the maximal jerk of speed curve, respectively. Note that there are two variables in one equation. Therefore, for a given s, a can be calculated using Equation (43). Discretized with interval of 0.01, s can be easily solved by exhaustive method. With the value of (s, a), the trajectory of CAV s can be obtained by Equation (41).

3) Trigonometry Method Combined With Rolling Horizon: Note that the trigonometry method ignores speed boundary and safety constraints, and the method assumes that the speed of preceding vehicle keeps as a constant value when the preceding vehicle is an HDV, which may lead to a negative speed, and cause crash among vehicles if the trigonometry method is only used once.

In that case, the trigonometry method combined with rolling horizon, also known as Model Predictive Control (MPC), is developed to avoid such issues. As shown in Figure 6, at time t_c^i , rolling horizon provides a full acceleration trajectory $G_n^i(t) = dv_n(t)/dt$ based on the trigonometry method at time period $[t_c^i, t_{sl,n}^i]$.

The joint acceleration $a_n^i(t), t \in [t_c^i, t_c^{i+1})$ is determined by the following equation:

$$a_{n}^{i}(t) = \begin{cases} a_{n}^{r,i}(t), & if \ v_{n}(t_{sl,n}^{i}) < 0, a_{n}^{r,i}(t) < \min \\ a_{n}^{v,i}(t), & \min_{t \in [t_{c}^{i}, t_{c}^{i+1})} \{G_{n}^{i}(t)\} \end{cases}$$

$$= \begin{cases} a_{n}^{v,i}(t), & \inf_{t \in [t_{c}^{i}, t_{c}^{i+1})} \{G_{n}^{i}(t)\} \\ a_{n}^{v,i}(t), & \min_{t \in [t_{c}^{i}, t_{c}^{i+1})} \{G_{n}^{i}(t)\} \end{cases}$$

$$G_{n}^{i}(t), \quad otherwise$$

$$(46)$$

where $a_n^{v,i}(t)$ is the car-following acceleration calculated by Equation (27), and $a_n^{r,i}(t)$ is the acceleration to avoid negative speed to the average speed (v_h^i) of the CAV, calculated by

$$a_n^{r,i}(t) = \max \left\{ a_{c,\min}, \frac{v_h^i - v_n(t_c^i)}{\Delta t} \right\}.$$

Without considering the lane change behavior of the CAV, the position and speed of CAV at time t ($t \in [t_c^i, t_c^{i+1})$) are determined as follows:

$$v_n(t) = \int_{t_c^i}^t a_n^i(t)dt, x_n(t) = \int_{t_c^i}^t v_n(t)dt$$
 (47)

F. A Novel Dynamic Bus Lane Control Strategy

As shown in Figure 1, the studied link has both GPL and DBL. Assume that CAVs can switch from the general-purpose lane to the bus lane to achieve high speeds while considering bus priority, and ensuring collision-free trajectories with their preceding and following vehicles in the bus lane. To simplify the problem, we assume instantaneous lane changing behavior, enabling CAVs to perform an economically efficient and collision-free longitudinal trajectory.

1) Trajectory With Fixed Final Speed of CAV in Bus Lane: Similar to CAEB, the terminal speed of CAVs is known with the target speed v_{tar} of CAVs in DBL. If the trigonometry method is adopted, it can use v_{tar} to calculate the values of (s, a). The trajectory is planned with two variables and two non-linear equations, which significantly increase the computational time, so the revised trajectory in DBL described as follows:

$$v'_{n}(t) = \begin{cases} v_{tar} + v_{d} \cos(st), & t \in \left[t_{c}^{i}, t_{c}^{i} + \frac{\pi}{2s}\right) \\ v_{tar}, & t \in \left[t_{c}^{i} + \frac{\pi}{2s}, t_{f,n}'\right] \end{cases}$$
(48)

where t_c^i is the current time for *i*-th rolling horizon. v_d is the difference speed between the current speed $v(t_c^i)$ and the target speed v_{tar} is calculated by $v_d = v(t_c^i) - v_{tar}$. $t_{f,n}^i$ is the terminal time that the CAV passes through the intersection.

Compared with Equation (41), one of trigonometry speed curves is deleted, v_h is replaced by v_{tar} , and $t_{sl,n}$ is replaced by a variable $t'_{f,n}$. There are two variables in the speed curve. And the variables can be determined as below:

$$\max_{s \in \{0,1\}} \{s\} \tag{49}$$

Subject to:
$$\int_{t^i}^{t'_{f,n}} v_n(t)dt = D_{tot} - x(t_c^i)$$
 (50)

Acceleration and jerk constraints(44), (45)

(51)

Equation (50) states that the CAV must pass through the intersection at time $t'_{f,n}$. $(s, t'_{f,n})$ can still be solved by discretizing s, and position $x'_n(t)$ and speed $v'_n(t)$ of CAV during the time period $t \in [t^i_c, t'_{f,n}]$ in DBL can be obtained by solving Equations (47) and (48).

2) Lane Changing Criteria and Trajectory of CAV in DBL: We assume that the ego CAV will engage in lane-changing behavior and merge into the DBL provided that its trajectory meets the safety conditions with respect to the vehicles ahead

and behind it within the DBL, and the time that the ego CAV passes the stop line must at green or yellow phase. The constraints are formulated as follows:

$$x'_{n}(t) - x'_{n-f}(t) \ge \tau v'_{n-f}(t)$$
 (52)

$$x'_{n,p}(t) - x'_n(t) \ge \tau v'_n(t)$$
 (53)

$$\left[\frac{t'_{sl,n}}{t_{cyc}}\right]t_{cyc} - t'_{sl,n} \ge t_{red} \tag{54}$$

where $x_{n,f}'(t), v_{n,f}'(t)$ are the positions and speeds of the following vehicles in DBL, respectively. $x_{n,p}'(t), v_{n,p}'(t)$ are the positions and speeds of the preceding vehicles in DBL, respectively. $t_{sl,n}'$ is the time of the ego CAV passing the stop line in DBL.

Equation (52) and Equation (53) state the current CAV keeps the safety headway with its preceding and following vehicles in DBL at all time. Equation (54) means CAV passing through intersection without stop.

In our study, the lane changing acceleration benefit results in the motivation of CAV lane changing behaviors, when the acceleration benefit Δa_n is larger than threshold a_{th} . The formulation for Δa is shown as follows:

$$\Delta a_n = a'_n(t_c^i) - a_n(t_c^i) > a_{th}$$
 (55)

where $a'_n(t^i_c)$ is the maximum acceleration in DBL at next rolling horizon time window, equal to $a'_n(t^i_c) = \max_{t \in [t^i_c, t^{i+1}_c)} dv'_n(t)/dt$. $a_n(t^i_c)$ is the acceleration in GPL, which is determined by Equation (46).

If the above conditions are satisfied, the current CAV can make a lane change to DBL. For the eco-driving strategy of CAEBs and CAVs, and the control strategy of DBLs, a system diagram is developed to explain the process of all vehicles driving in the road section with a bus stop and a signalized intersection, as shown in Figure 7.

The control center collects current SPaT information, and the time period t_{last} (i.e., time to red phase). When a new vehicle is driving into the intersection, the controller verifies the type of the entry vehicle. If the vehicle is an HDV, its trajectory will be generated by IDM. If the vehicle is a CAEB, its trajectory will be designed by the proposed bi-level programming, and CAEB will receive the proposed trajectory and driving through the intersection. If the vehicle is a CAV, in each simulated time step, the control center determines the acceleration curve in GPL using the revised eco-driving strategy firstly, and then the proposed DBL strategy to verify that whether the CAV will take the lane changing behavior to bus lane or not.

III. NUMERICAL EXPERIMENTS

In this section, we first setup the simulation environment in MATLAB. Then, the results of bus trajectory planning are explored. The results of eco-driving of CAVs are discussed considering different market penetrate rates. Finally, the benefits of DBL control strategy are analyzed.

A. Simulation Setup

Numerical simulations are conducted in MATLAB 2019A with a 2.4 GHz Intel (R) Core (TM) i5-9300H and 16.0 GB

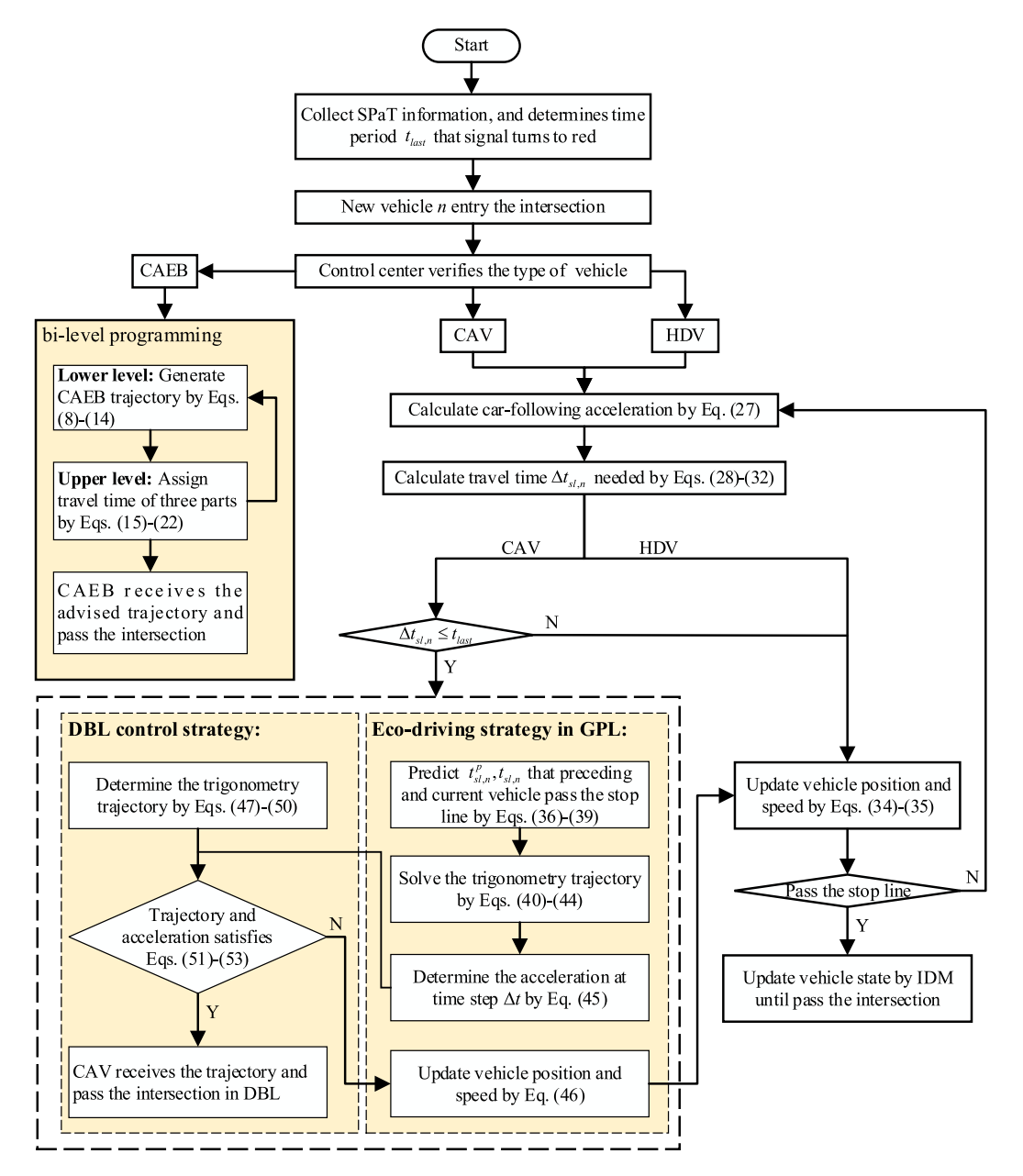


Fig. 7. Control scheme of vehicles under partially connected vehicle environment.

RAM. A simple roadway with one bus lane and one general purpose lane is selected as the case study, shown in Figure 1. The bus stop has the capacity of two buses to dwell at the same time. The values of the parameters used in this study are given in Table I. We start with a benchmark scenario: (1) the demand of general traffic is 720 veh/h; (2) the target speed of CAVs in DBL is 13.3 m/s; (3) the arrival interval of cars is constant without variance; (4) the distance between entry and bus stop is 150 m; (5) the buffer length is 50 m, where the lane changing behaviors of CAVs are prohibited; and (6) the threshold of acceleration benefit is 1.0 m/s². Sensitivity analysis will be conducted in the next section to evaluate the significant impacts of multiple external factors on DBL control strategy.

B. Results of Bus Trajectory Planning

In this study, to show the impacts of traffic signals phase and timing, we assume that the arrival time interval of two consecutive CAEBs is random, and the planned trajectories of CAEBs are depicted in Figure 8. Considering the joint effects of bus stops and signalized intersections, all CAEBs can pass the intersection without additional stopping, resulting in about 30-50% energy savings, and 1-6% travel time savings [6]. Meanwhile, this figure shows that there are available spatial-temporal gaps for other vehicles to take advantage while still ensuring the bus priority.

C. Results of Eco-Driving of CAVs

Figure 9 illustrates the spatio-temporal trajectories of CAVs and HDVs in a GPL, depicting the operation performance of general traffic under varying CAV Market Penetration Rates (MPRs). To obtain these results, we combine our proposed revised trigonometry method with rolling horizon. The black lines depict the trajectories of HDVs, and the blue lines denote the trajectories of CAVs.

TABLE I
SIMULATION PARAMETERS SETUP

Parameter	value
Road parameters	
Length of buffer D_{cl} (m)	50
Length between entry and bus station D_{bs} (m)	150
Length between bus station and stop line D_{sl} (m)	250
Length of intersection D_{tot} (m)	450
Road slope θ (rad)	0
Gravity acceleration g (m/s²)	9.81
Volume of cars Q_{car} (veh/h)	720
Volume of buses Q_{bus} (veh/h)	60
Signal Phase information	
Length of signal cycle t_{cyc} (s)	60
Length of green phase t_{gre} (s)	30
Length of yellow phase t_{yel} (s)	3
Length of red phase t_{red} (s)	27
Lost time at the beginning of green phase t_{ls} (s)	3
Bus energy consumption model	
Mass of a CAEB M (kg)	14515
Aerodynamic resistance coefficient k (kN/m·s ²)	0.00386
Rolling resistance coefficient f_{rl}	0.009
Equivalent factor cc (kJ/s)	6
Efficiency coefficient η , η_{wl} , η_{fd} , η_{mot} , η_{batt} 0.95, 0.	92, 0.97, 0.98, 0.99
Vehicle energy consumption model	
mass of a CAV or HDV m (kg)	1266
Car rolling resistance b_1 (kN)	0.333
Car aerodynamic drag coefficient b ₂ (kN)	0.00108
idling gasoline consumption rate \bar{a} (ml/s)	0.444
Engine energy efficiency coefficient β_1 (ml/kJ)	0.09
Gasoline consumption coefficient β_2 (kJ/ml·m·s ²)	0.04
Coefficient gasoline converts to electricity ρ_c (kJ/ml)	31.25
Variables in CAEB Trajectory Planning	
Bus dwelling time tw (s)	20
Length of bus l_b (m)	14
Terminal speed of CAEB v_e (m/s)	18.0
Limit speed of CAEB $v_{b,\text{max}}$ (m/s)	18.0
Upper bound of CAEB acceleration $a_{b,\text{max}}$ (m/s ²)	1.5
Lower bound of CAEB acceleration $a_{b,min}$ (m/s ²)	-2.0
Variables in CAV eco-driving and IDM parameters	
Safety time headway of vehicle τ (s)	1.6
Saturation time headway of car (s)	2.0
Minimum safety gap s_0 (m)	2.0
Length of car l_c (m)	6.0
Limit speed of vehicle $v_{c,\text{max}}$ (m/s)	18.0
Eco cruising speed v_{eco} (m/s)	13.3
Target speed in bus lane v_{tar} (m/s)	13.3
The threshold of acceleration benefit a_{th} (m/s ²)	1.0
Upper bound of CAEB acceleration $a_{c,\text{max}}$ (m/s ²)	2.5
Desired deceleration of HDV $a_{c,d}$ (m/s ²)	2.0
Lower bound of CAEB acceleration $a_{c,min}$ (m/s ²)	-4.0
Limit changing rate of acceleration k_{max} (m/s ³)	10.0
Variables in initial condition	
Initial speed of buses and cars v_s (m/s)	10.0

In Figure 9, it can be observed that HDVs may come to a stop before the intersection stop line due to the red signal, creating a shock wave that leads to increased travel time and

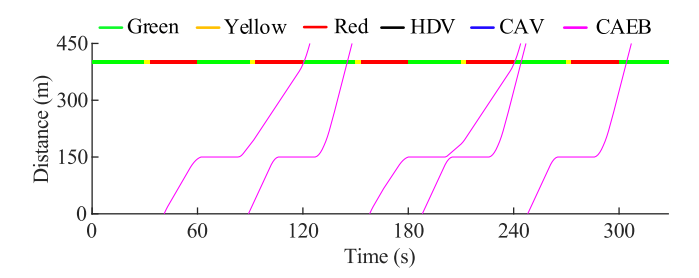


Fig. 8. Spatio-temporal trajectories of CAEB in bus lane.

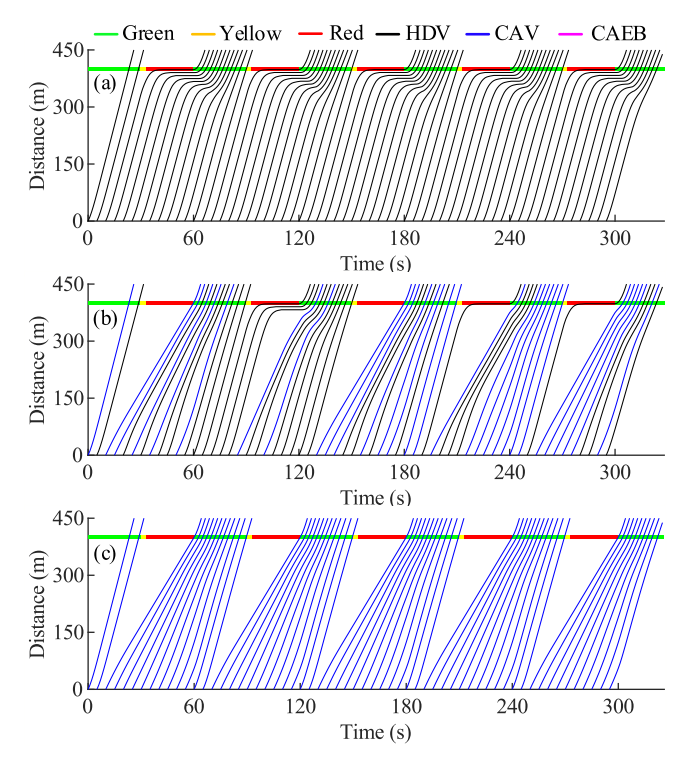


Fig. 9. Spatio-temporal trajectories of vehicles in GPL under partially CAV environment: (a) MPR = 0%, (b) MPR = 50%, (c) MPR = 100%.

energy consumption. This occurs because HDVs are unable to receive and use SPaT information for eco-driving. On the other hand, CAVs can utilize SPaT and RSUs information to execute eco-driving strategies and pass through the intersection without stopping. Additionally, it is noteworthy that other HDVs can follow the trajectories of CAVs and drive through the intersection smoothly, thereby reducing the impact of the shock wave and startup lost time in the heterogeneous traffic flow. Consequently, the overall energy consumption and travel time of general traffic can be reduced, as illustrated in Table II.

Table II shows the average travel time and energy consumption under the different MPRs. The baseline scenario is the penetration rate with zero. Numerical results indicate that both the vehicle travel time and energy consumption show a decreasing trend with the increase of MPR. When the MPR is equal to 100%, the average vehicle travel time decreases by 5.4%, while the vehicle energy consumption falls by 36.8% from about 5486.4 kJ to 3468.2 kJ. Thus, the eco-driving control strategy of CAVs can smooth the general traffic flow notably, resulting in much energy savings and travel efficiency improvement. In addition, the average computational time of

TABLE II
TRAVEL TIME AND ENERGY CONSUMPTION OF GENERAL TRAFFIC

CAV MPRs (%)	Travel time (s)	Reduction (%)	Energy consumption (kJ)	Reduction (%)
0	42.7	0.0	5486.4	0.0
20	42.0	1.5	4819.6	12.2
40	41.6	2.4	4279.4	22.0
60	41.2	3.4	3836.8	30.1
80	40.8	4.3	3585.0	34.7
100	40.4	5.4	3468.2	36.8

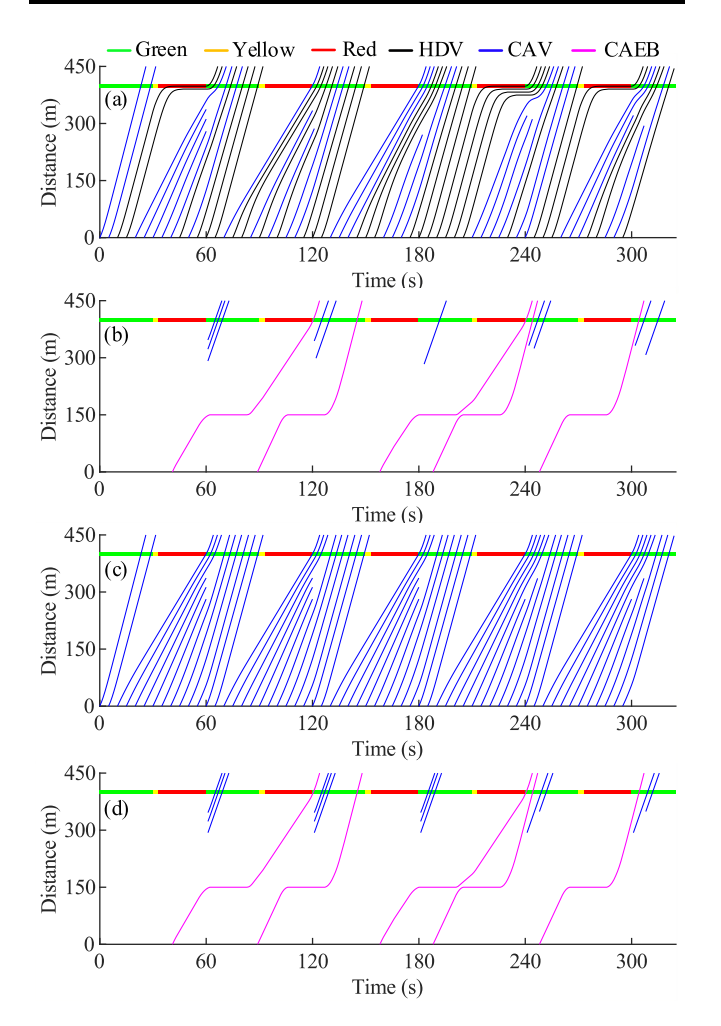


Fig. 10. Spatio-temporal trajectories of vehicles with DBL strategy: (a) MPR = 50% GPL, (b) MPR = 50% DBL, (c) MPR = 100% GPL, (d) MPR = 100% DBL.

CAVs for each rolling horizon is 15 ms, which implies that our proposed eco-driving strategy can be potentially used for real-world implementation.

D. Results of DBL Control Strategy

Based on our proposed novel DBL control strategy, the CAVs are allowed to use the bus lane without compromising the bus priority. Figure 10 shows the spatio-temporal trajectories of all vehicles under different CAV MPRs with eco-driving of CAVs in GPL and the novel DBL control strategy. As shown in Figure 10 (a) and (c), the preceding vehicles in GPL can

TABLE III

TRAVEL TIME AND ENERGY CONSUMPTION BY DBL STRATEGY AND ECO-DRIVING STRATEGY IN GPL

CAV MPRs (%)	Travel time (s)	Reduction (%)	Energy consumption (kJ)	Reduction (%)
0	42.7	0.0	5486.4	0.0
20	41.3	3.3	4709.0	14.2
40	40.1	6.0	4122.7	24.9
60	39.5	7.3	3767.6	31.3
80	39.0	8.6	3522.1	35.8
100	38.7	9.3	3467.8	36.8

pass the stop line earlier compared with the trajectory results in Figure 9 (b) and (c) due to some CAVs changing into the DBL, and the average speed of HDVs is close to the ecodriving speed, resulting in the decrease of vehicle travel time and energy consumption. Meanwhile, it can be found that there are no conflicts between CAEBs and CAVs in DBL. And the target traveling speed of CAVs in DBL is set as the value of eco-driving speed, resulting in much energy savings.

Table III presents the average vehicle travel time and energy consumption under various CAV MPRs using both DBL and eco-driving strategies. The numerical outcomes indicate that the average travel time and energy consumption exhibit a decreasing trend as the MPRs increase. Moreover, the combined approach of DBL and eco-driving in GPL outperforms the outcomes of the eco-driving strategy alone, as shown in Table II and Table III. For instance, when the MPR is 100%, the use of DBL results in a 9.3% reduction in travel time, nearly double the reduction obtained from the eco-driving strategy alone. Additionally, the energy consumption reduction exceeds 36.8% by using DBL. These simulation findings demonstrate that our proposed DBL control strategy can further improve vehicle efficiency, reduce energy consumption, increase road resource utilization, and mitigate traffic congestion in GPL.

IV. SENSITIVITY ANALYSIS

In this section, sensitivity analyses are conducted to quantify the impacts of related variables on the performance of DBL control strategy, including the target speed of CAVs in DBL, the heterogeneous traffic flow, the random arrival interval of cars, the position of the bus stop, the volume of general traffic, the buffer length, and acceleration benefit threshold of lane changing behaviors.

A. Sensitivity to Target Speed of CAVs in DBL

The target speed of CAVs in DBL plays a crucial role in determining the planned trajectories, ultimately affecting the vehicle's travel time and energy consumption. To examine the impact of the target speed, two scenarios with different target speeds are conducted: eco-driving speed and maximum speed. The performance of the DBL strategy is evaluated using four indicators: the proportion of travel time reduction, the proportion of energy consumption reduction, the lane changing proportion of total vehicles, and the lane changing proportion

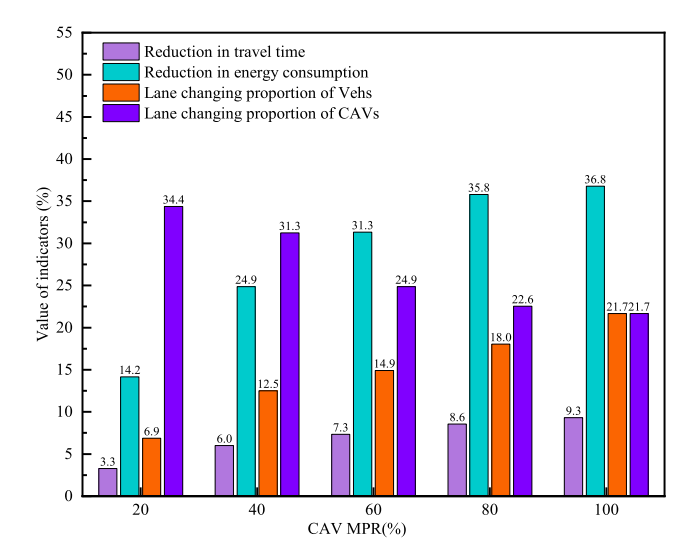


Fig. 11. Simulation results with the eco-cruise speed of v_{eco} .

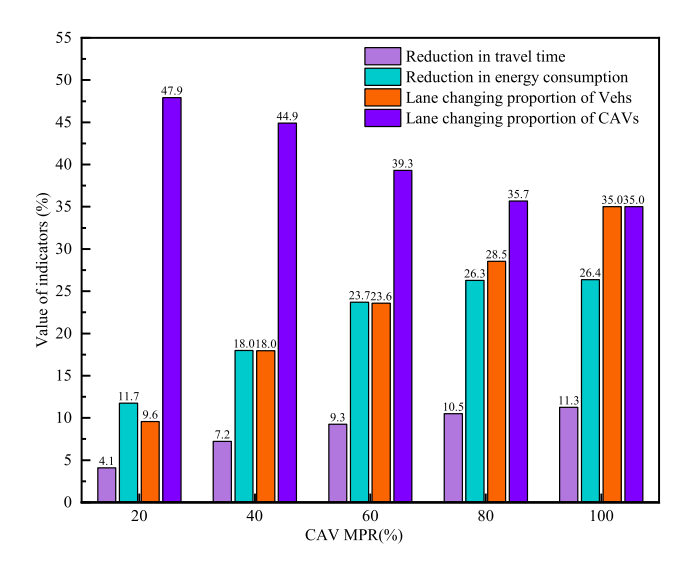


Fig. 12. Simulation results with the target speed of $v_{c,\text{max}}$.

of total CAVs. The simulation results of these two scenarios with the DBL control strategy under different MPRs are presented in Figure 11 and Figure 12.

The simulation results reveal that the lane changing proportions in the maximal speed scenario are greater than those in the eco-cruise speed scenario. Due to the speed difference, the acceleration benefits obtained from the maximum speed calculated by Equation (55) consistently outweigh the benefits of eco-cruise speed, resulting in a greater number of lane-changing maneuvers. Consequently, the higher traveling speed of CAVs in DBL with more lane changing behaviors leads to better travel time reduction results with the maximum speed compared to the eco-driving speed results. For instance, in 100% MPR, the travel time reduction achieved with the maximum speed is 11.3%, while the reduction obtained with the eco-cruise speed is less than 10%. However, the results for vehicle energy consumption show that the eco-cruise speed scenario outperforms the maximal speed scenario.

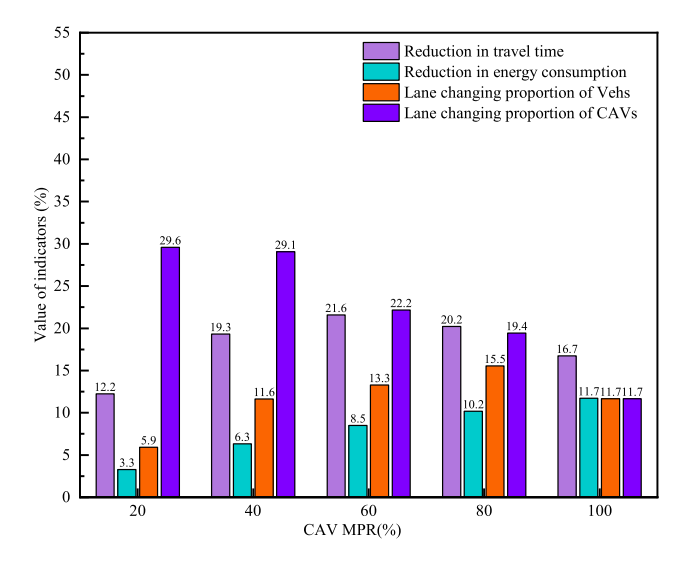


Fig. 13. Simulation results with the heterogeneous characteristic of traffic.

B. Sensitivity to Heterogeneous Characteristic of Traffic Flow

In the real-world, considering the heterogeneous of traffic flow, the speed limitation for buses and cars is different, and the headway should be different for CAVs and HDVs. Therefore, a sensitivity analyses to the heterogeneous of traffic flow has been added to discuss the performance of our proposed DBL control strategy. In the simulation, the upper speed limitation of buses is set to 15 m/s (54 km/h), and the safe time headway for HDVs is set to 1.6s, the headway for CAVs is set to 1.3 s (CAV following HDV) and 0.9 s (CAV following CAV). The results are illustrated in Figure 13. Results reveal that the savings of travel time in the heterogeneous traffic scenario are larger than those in the homogeneous scenario (Table III). Due to the safety time headway difference, within the high CAV PR condition, the car-following acceleration of CAVs in GPL calculated by Equation (27) consistently outweigh the acceleration from homogeneous scenario, resulting in a greater travel speed and a short travel time. Furthermore, the larger value of acceleration in GPL also decreases the lane changing benefit calculated by Equation (55), thereby the lane changing proportions of heterogeneous scenario perform a smaller value in comparison to homogeneous scenario. However, due to the larger acceleration of CAVs, the savings of fuel consumption in heterogeneous are smaller than those in homogeneous scenario, and even show a decrease trend at the high CAV MPR (still outperforms the non-CAV condition).

C. Sensitivity to Random Arrival Interval of Cars

In this section, the sensitivity analysis of random arrival interval of cars is added to perform the effectiveness of the proposed DBL control strategy under stochastic environment. In the simulation, travel demand is set as 720 veh/h, and the MPR rate is set to be 40%. The arrival interval of cars forms a Gaussian distribution with a mean value of 5 s (3600/720). We vary the stand variance of the Gaussian distribution between 0 and 1 s with an increment of 0.1 s. The experiment result is illustrated in Figure 14. Figure 14 demonstrates that the benefits of our proposed strategy decrease

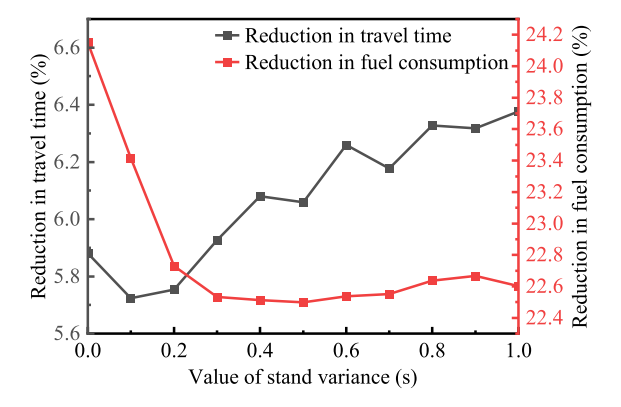


Fig. 14. Simulation results under stochstic environment.

in fuel consumption as stand variance grows, whereas the savings in travel time shows an increase trend. The reason is that under uncongested traffic, a greater variance outcome a larger probability to reduce the start-up time loss of the queued vehicles, and thus reduce the idling time of subsequent vehicles, resulting in an increase in travel time saving with the increase in variance. However, the reduction in travel time also reduces the abrupt acceleration and deceleration behavior of the vehicles, leading to a downward trend in fuel consumption savings rate as the variance increases.

D. Sensitivity to Position of the Bus Stop

In this section, the sensitivity analysis is performed to discuss the influence of bus station position. In the simulation, travel demand is set as 720 veh/h, and the MPR rate is set as 100%. Two cases with different position of bus stop are tested. Spatio-temporal trajectories of vehicles in the two cases are displayed in Figure 15. Combined with Figure 10 (c) and (d), it is found that, as the distance between the entry and bus station increases, the dwelling time of CAEB at bus station grows to prevent the additionally idling at the stop line of intersection, which condenses the available time of green and yellow phase, resulting in the decrease of lane changing proportions.

E. Sensitivity to Demand of General Traffic in GPL

The volumes of general traffic (Q_{veh}) are set as 480, 720, 960 veh/h to represent different levels of traffic demand in GPL. The simulation results of four factors under the different volumes in GPL and different MPRs are shown in Figure 16. Results show that all the four indicators increase with the increase of traffic volume, indicating that our proposed novel DBL control strategy has better performance under the condition of high traffic volume, resulting in much more energy savings. Specifically, under the low traffic demand condition with the volume of 480 veh/h, the CAVs can get an acceptable speed near to the eco-cruise speed, without frequent lane changing behaviors to pursue high speed. Consequently, the lane changing proportion of CAVs remains low (13%), resulting in lower reductions in energy consumption and travel time compared with the simulation results of the scenario with the volume of 720 veh/h at the same CAV MPR.

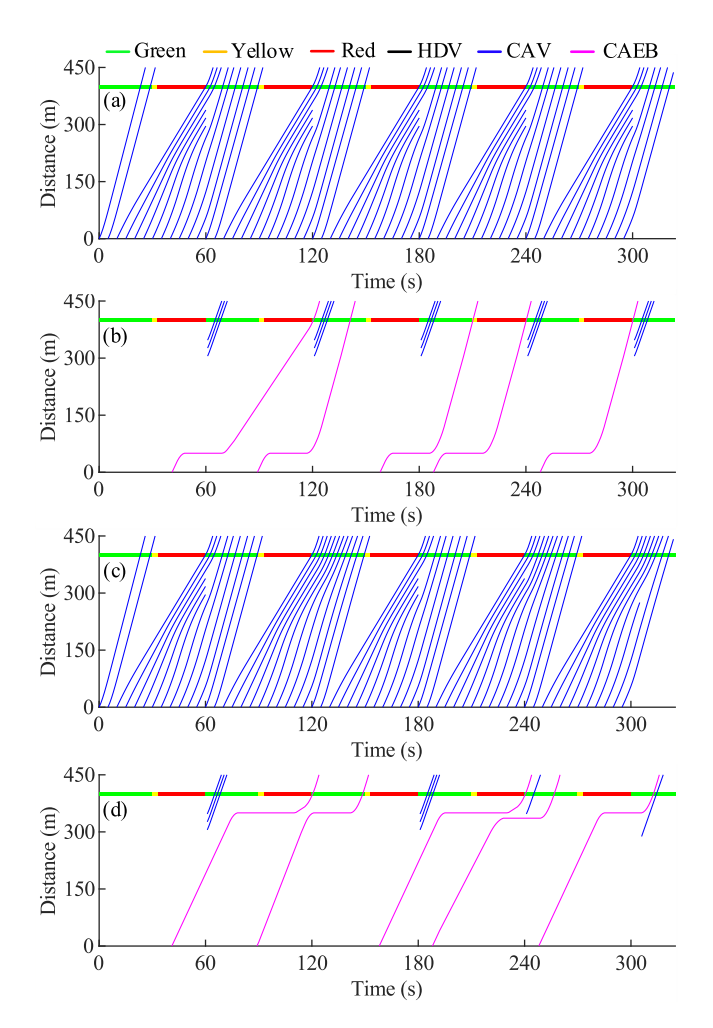


Fig. 15. Spatio-temporal trajectories of vehicles under different bus stop position: (a) $D_{bs}=50~\mathrm{m}$ GPL, (b) $D_{bs}=50~\mathrm{m}$ DBL, (c) $D_{bs}=350~\mathrm{m}$ GPL, (d) $D_{bs}=350~\mathrm{m}$ DBL.

Under the high traffic demand with the volume of 960 veh/h, when the MPR is 20%, results show that more than 60% CAVs drive into the DBL, resulting in the energy savings of 30.4% and travel time reduction of 32.7%. Meanwhile, when the MPR is 100%, over 35% CAVs select to drive into the DBL, resulting in more than 50% energy savings and 40% traveling time reduction and mitigation of the traffic congestion in GPL. Considering the saturation headway of general traffic t_{hw} being 2 s, the saturation flow is 1800 veh/h. On average, the number of vehicles arriving in one signal cycle is 16 (i.e., 960×60.3600). Vehicles passed maximal in one signal cycle are 15 (1800 \times 30.3600). The number of vehicle arrivals is larger than the road capacity, which causes a waiting queue formed at the signalized intersection, significantly increasing the vehicles' travel time. Meanwhile, lane changing behaviors of CAVs can reduce the total volume of vehicles in GPL, resulting in the alleviation of congested traffic, which can lead to the significant energy and traveling time savings in GPL.

F. Sensitivity to Buffer Length and Acceleration Benefit Threshold

Both of the buffer length and acceleration benefit threshold have important impacts on the performance of the novel

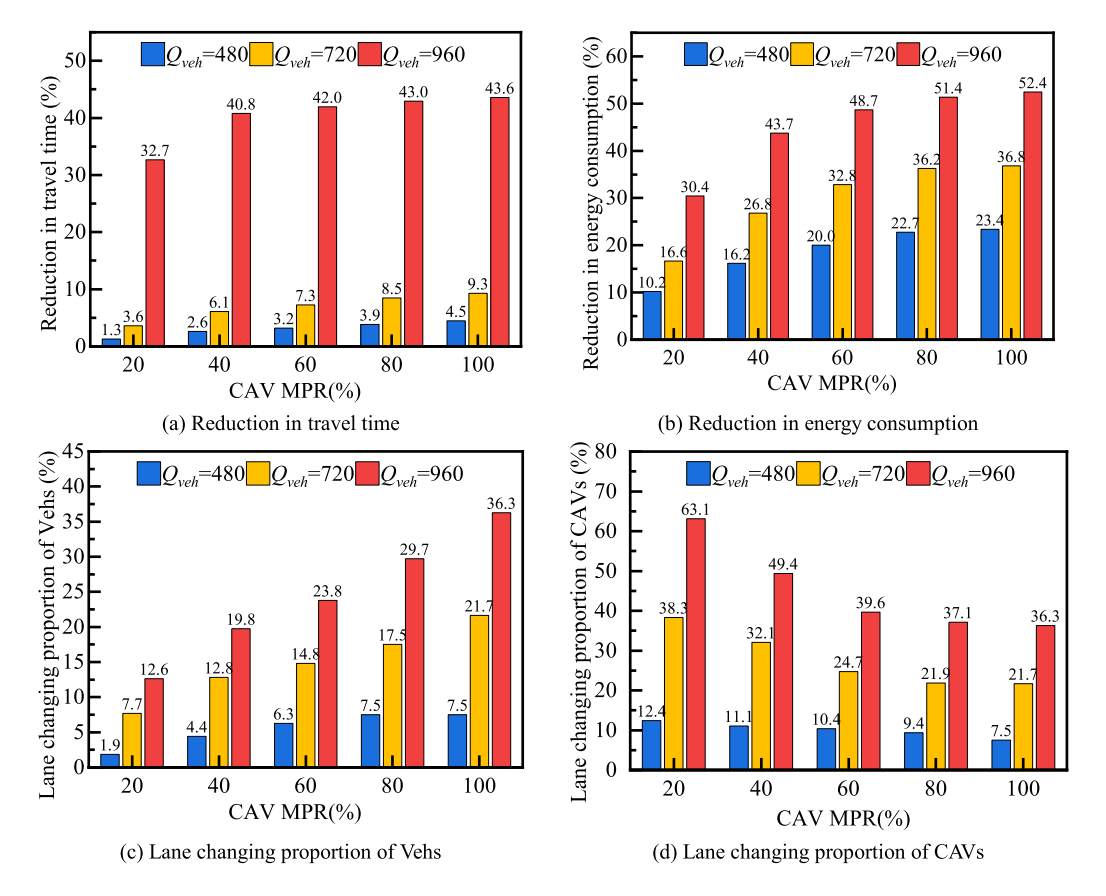


Fig. 16. Simulation results of different volumes in GPL.

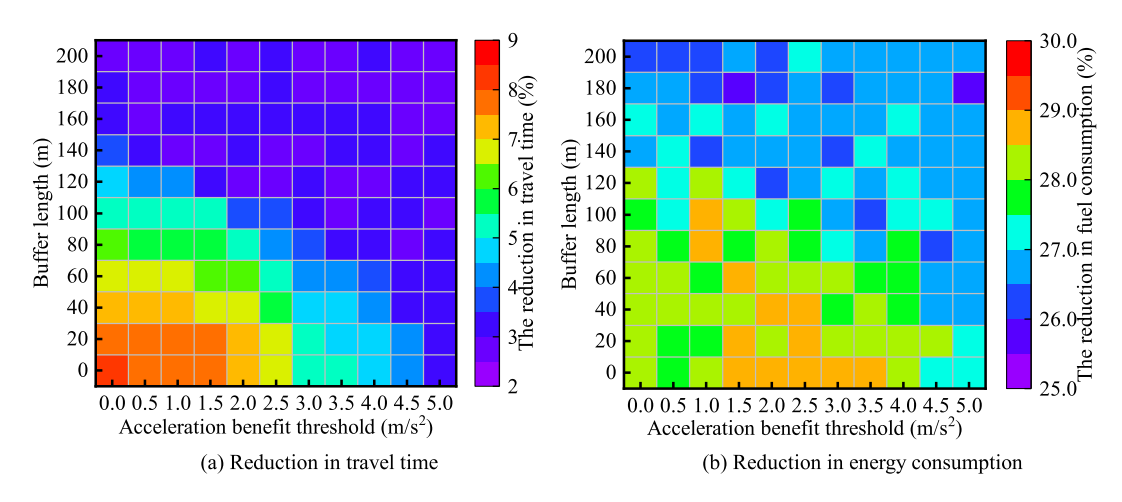


Fig. 17. Simulation results of different buffer lengths and acceleration thresholds under 50% MPR.

DBL control strategy, as the buffer length limits the lane changing behavior area of CAVs, and the acceleration benefit threshold triggers lane changing behaviors of CAVs. Thus, the two factors are combined to analyze the benefits of vehicle energy consumption and travel time under the different MPRs. Figure 17 and Figure 18 show the simulation results of the energy savings and travel time reduction of vehicles under the different buffer lengths from zero to 200 m, and acceleration benefit threshold from 0 to 5.0 m·s⁻² under 50% MPR and 100% MPR.

Overall, the travel time shows an increasing trend with the increase of buffer length and acceleration benefit threshold due to the limitations of lane changing behaviors. When the buffer length and acceleration threshold are zero, the proportion of travel time reduction is around 9% under 50% MPR. For vehicle energy consumption, the optimal combination of the two parameter of maximum energy savings is 60 m and 1.5 m/s², with the proportion of energy savings around 30%. Under 100% MPR, the best acceleration benefit threshold is 2.5 m/s², with the buffer length from zero to 60m, resulting in

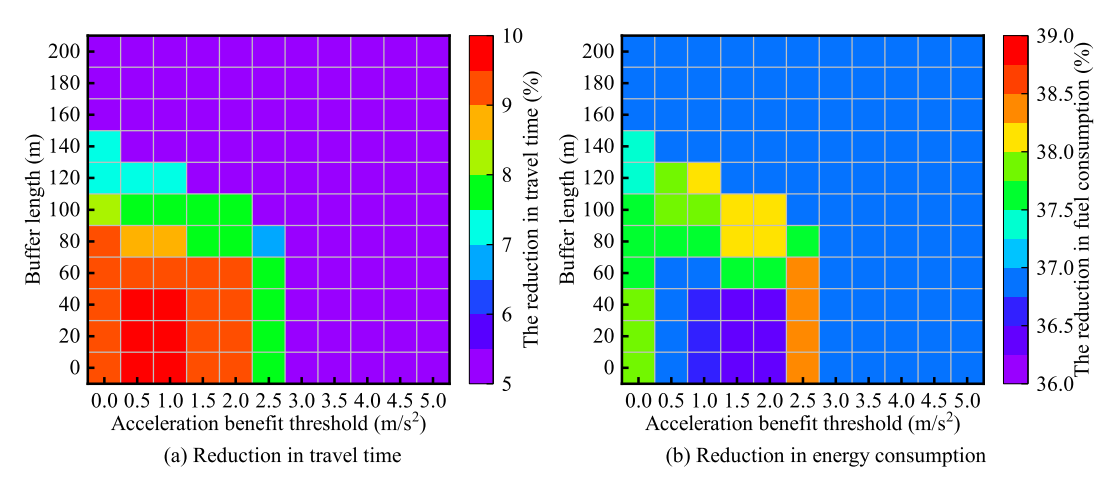


Fig. 18. Simulation results of different buffer length and acceleration threshold under 100% MPR.

the energy savings around 38%. Meanwhile, for the maximum travel time reduction, the acceleration benefit threshold is 0.5 m/s² or 1 m/s², with the buffer length from zero to 40 m.

V. CONCLUSION

This study develops a new DBL control strategy of eco-driving under partially connected vehicle environment to mitigate the general traffic in GPL and improve the utilization of bus lanes. More specially, the trajectory planning method of CAEBs is introduced with consideration of the joint effects of bus stops and signalized intersections. An eco-driving strategy of CAVs in GPL is proposed based on the revised trigonometry method. Then the new DBL control strategy is developed with combing the planned trajectories of CAVs and CAEBs in the context of bus priority. Numerical experiments indicate that the new DBL control strategy has higher performance compared with the benchmark strategies. Overall, both of the average energy consumption and travel time show a decreasing trend with the increase of MPRs. Results show that the energy savings could be around 16%-41% under different CAV MPRs, with the travel time reduction of about 4%-10%.

Sensitivity analysis is conducted to explore the kernel parameters on the impacts of operation performance in GPL with our proposed new DBL control strategy. For the target speed of CAVs in DBL, we find that the travel time reduction with the maximum speed shows better performance compared with the results of the eco-driving speed. And the savings of travel time in the heterogeneous traffic scenario are larger than those in the homogeneous scenario. Inversely, the savings of fuel consumption are smaller than those in homogeneous scenario. With considering the impact of random arrival interval of cars, results show that the savings in travel time shows an increase trend with the increase of stand variance, while the fuel consumption savings show a descending trend. Our proposed DBL strategy also shows good performance to the different positions of the bus stop. As for the volume of general traffic in GPL, results show that the new DBL has good flexibility with the increase of travel volume. For the combination of buffer length and the acceleration threshold, the proportion of travel time reduction can be increased with the increase of these two parameters. Meanwhile, the vehicle

energy savings shows fluctuation features with the increase of two parameters. The two parameters are 60 m and 1.5 m/s² under 50% MPRs, resulting in the maximum energy savings around 30%. Thus, there is optimal combination of such two parameters.

In this study, we do not take into account the potential impact of signal priority on the trajectory planning of CAEBs since we assume the fixed-time traffic signals. Moreover, we only consider a scenario where there are two lanes, namely the DBL and GPL, resulting in a limited scenario of lane changing of CAVs (i.e., only to the DBL). Therefore, future studies should include investigation of the effects of signal priority on CAEB trajectory planning and explore more sophisticated scenarios as well as advanced eco-driving methods to optimize the entire traffic operation.

REFERENCES

- [1] S. G. Li and Y. F. Ju, "Evaluation of bus-exclusive lanes," *IEEE Trans. Intell. Transp. Syst.*, vol. 10, no. 2, pp. 236–245, Jun. 2009.
- [2] L. T. Truong, M. Sarvi, and G. Currie, "Exploring multiplier effects generated by bus lane combinations," *Transp. Res. Rec., J. Transp. Res. Board*, vol. 2533, no. 1, pp. 68–77, Jan. 2015.
- [3] T. De Ceunynck et al., "Sharing is (s)caring? Interactions between buses and bicyclists on bus lanes shared with bicyclists," *Transp. Res. F, Traffic Psychol. Behav.*, vol. 46, pp. 301–315, Apr. 2017.
- [4] J. Zhao and X. Zhou, "Improving the operational efficiency of buses with dynamic use of exclusive bus lane at isolated intersections," *IEEE Trans. Intell. Transp. Syst.*, vol. 20, no. 2, pp. 642–653, Feb. 2019.
- [5] J. Hu, Z. Zhang, Y. Feng, Z. Sun, X. Li, and X. Yang, "Transit signal priority enabling connected and automated buses to cut through traffic," *IEEE Trans. Intell. Transp. Syst.*, vol. 23, no. 7, pp. 8782–8792, Jul. 2022.
- [6] X. Shan, C. Wan, P. Hao, G. Wu, and X. Zhang, "Connected eco-driving for electric buses along signalized arterials with bus stops," *IET Intell. Transp. Syst.*, vol. 17, no. 3, pp. 579–591, Mar. 2023.
- [7] Z. Wang, G. Wu, and M. J. Barth, "Cooperative eco-driving at signalized intersections in a partially connected and automated vehicle environment," *IEEE Trans. Intell. Transp. Syst.*, vol. 21, no. 5, pp. 2029–2038, May 2020.
- [8] A. S. Shalaby, "Simulating performance impacts of bus lanes and supporting measures," *J. Transp. Eng.*, vol. 125, no. 5, pp. 390–397, Sep. 1999.
- [9] Y. Z. Farid, E. Christofa, and J. Collura, "Dedicated bus and queue jumper lanes at signalized intersections with nearside bus stops: Personbased evaluation," *Transp. Res. Rec., J. Transp. Res. Board*, vol. 2484, no. 1, pp. 182–192, Jan. 2015.

- [10] M. Shen, W. Gu, S. Hu, and H. Cheng, "Capacity approximations for near- and far-side bus stops in dedicated bus lanes," *Transp. Res. B, Methodol.*, vol. 125, pp. 94–120, Jul. 2019.
- [11] H. Cui, K. Xie, B. Hu, H. Lin, and R. Zhang, "Analysis of bus speed using a multivariate conditional autoregressive model: Contributing factors and spatiotemporal correlation," *J. Transp. Eng., A, Syst.*, vol. 145, no. 4, Apr. 2019.
- [12] J. Viegas and B. Lu, "Widening the scope for bus priority with intermittent bus lanes," *Transp. Planning Technol.*, vol. 24, no. 2, pp. 87–110, Jan. 2001.
- [13] H. Yang and W. Wang, "An innovative dynamic bus lane system and its simulation-based performance investigation," in *Proc. IEEE Intell.* Vehicles Symp., Jun. 2009, pp. 105–110.
- [14] W. Wu, L. Head, S. Yan, and W. Ma, "Development and evaluation of bus lanes with intermittent and dynamic priority in connected vehicle environment," *J. Intell. Transp. Syst.*, vol. 22, no. 4, pp. 301–310, Jul 2018
- [15] M. Szarata and P. Olszewski, "Traffic modelling with dynamic bus lane," in *Proc. 6th Int. Conf. Models Technol. Intell. Transp. Syst. (MT-ITS)*, Jun. 2019, pp. 1–8.
- [16] A. Kampouri, I. Politis, and G. Georgiadis, "A system-optimum approach for bus lanes dynamically activated by road traffic," Res. Transp. Econ., vol. 92, May 2022, Art. no. 101075.
- [17] M. Xie, M. Winsor, T. Ma, A. Rau, F. Busch, and C. Antoniou, "Parameter sensitivity analysis of a cooperative dynamic bus lane system with connected vehicles," *Transp. Res. Rec., J. Transp. Res. Board*, vol. 2676, no. 1, pp. 311–323, Jan. 2022.
- [18] Y. Luo, J. Chen, S. Zhu, and Y. Yang, "Developing the dynamic bus lane using a moving block concept," *Transp. Res. Rec.*, *J. Transp. Res. Board*, vol. 2677, no. 1, pp. 1430–1443, Jan. 2023.
- [19] H. Yang and K. Oguchi, "Development and evaluation of connected-vehicle-enabled optimal dynamic path planning with bus stops," *Transp. Res. Rec., J. Transp. Res. Board*, vol. 2677, no. 1, pp. 577–586, Jan. 2023.
- [20] K. Othman, A. Shalaby, and B. Abdulhai, "Dynamic bus lanes versus exclusive bus lanes: Comprehensive comparative analysis of urban corridor performance," *Transp. Res. Rec., J. Transp. Res. Board*, vol. 2677, no. 1, pp. 341–355, Jan. 2023.
- [21] D. Biggs and R. Akcelik, "An energy-related model of instantaneous fuel consumption," *Traf. Eng. Con.*, vol. 27, no. 6, pp. 320–325, Jun. 1986.
- [22] M. Yu and J. Long, "An eco-driving strategy for partially connected automated vehicles at a signalized intersection," *IEEE Trans. Intell. Transp. Syst.*, vol. 23, no. 9, pp. 15780–15793, Sep. 2022.
- [23] F. Ye, P. Hao, G. Wu, D. Esaid, K. Boriboonsomsin, and M. Barth, "An advanced simulation framework of an integrated vehicle-powertrain ecooperation system for electric buses," in *Proc. IEEE Intell. Veh. Sym.*, Jun. 2019, pp. 2080–2085.
- [24] M. Treiber, A. Hennecke, and D. Helbing, "Congested traffic states in empirical observations and microscopic simulations," *Phys. Rev. E, Stat. Phys. Plasmas Fluids Relat. Interdiscip. Top.*, vol. 62, no. 2, pp. 1805–1824, Aug. 2000.
- [25] H. Xia, K. Boriboonsomsin, and M. Barth, "Dynamic eco-driving for signalized arterial corridors and its indirect network-wide energy/emissions benefits," *J. Intell. Transp. Syst.*, vol. 17, no. 1, pp. 31–41, Jan. 2013.



Changxin Wan received the B.S. degree in transportation engineering from Hohai University in 2022, where he is currently pursuing the M.S. degree with the College of Civil and Transportation Engineering. His research interests include connected and automated vehicle, eco approach and departure, traffic signal control, and transportation simulation.



Peng Hao (Member, IEEE) received the B.S. degree in civil engineering from Tsinghua University in 2008 and the Ph.D. degree in transportation engineering from the Rensselaer Polytechnic Institute in 2013. He is currently an Assistant Research Engineer with the College of Engineering, Center for Environmental Research and Technology, University of California at Riverside, Riverside. His research interests include connected vehicles, eco-approach and departure, sensor-aided modeling, signal control, and traffic operations.



Guoyuan Wu (Senior Member, IEEE) received the Ph.D. degree in mechanical engineering from the University of California at Berkeley, Berkeley, in 2010. He is currently a Full Researcher and an Adjunct Professor with the Bourns College of Engineering—Center for Environmental Research and Technology (CE-CERT) and Department of Electrical and Computer Engineering, University of California at Riverside. His research interests include the development and evaluation of sustainable and intelligent transportation system (SITS) technolo-

gies, including connected and automated transportation systems (CATS), shared mobility, transportation electrification, the optimization and control of vehicles, traffic simulation, and emissions measurement and modeling. He serves as an Associate Editor for a few journals, including IEEE TRANSACTIONS ON INTELLIGENT TRANSPORTATION SYSTEMS, IEEE OPEN JOURNAL OF INTELLIGENT TRANSPORTATION SYSTEMS, and SAE International Journal of Connected and Automated Vehicles. He is also a member of a few Standing Committees of the Transportation Research Board (TRB). He is a recipient of 2020 Vincent Bendix Automotive Electronics Engineering Award and the 2021 Arch T. Colwell Merit Award.



Xiaonian Shan received the B.S. degree from Southeast University in 2012 and the Ph.D. degree in transportation planning and management from Tongji University in 2018. From 2015 to 2016, he was a Visiting Ph.D. Student with the Bourns College of Engineering—Center for Environmental Research and Technology (CE-CERT), University of California at Riverside. Since 2021, he has been an Associate Professor with the College of Civil and Transportation Engineering, Hohai University. He is the author of more than 16 refereed papers in

scholarly journals and conferences. His research interests include connected and automated vehicle, vehicle energy and emissions modeling, managed lane design, traffic operation management, and intelligent transportation systems.



Matthew J. Barth (Fellow, IEEE) received the B.S. degree in electrical engineering/computer science from the University of Colorado in 1984 and the M.S. and Ph.D. degrees in electrical and computer engineering from the University of California at Santa Barbara, Santa Barbara, in 1985 and 1990, respectively. He is currently the Yeager Families Professor with the College of Engineering, University of California at Riverside (UCR). He is a part of the Intelligent Systems Faculty in Electrical and Computer Engineering and he is also the Director for

the Center for Environmental Research and Technology (CE-CERT), UCR's largest multi-disciplinary research center. He joined UCR in 1991, conducting research in intelligent systems. His current research interests include ITS and the environment, transportation/emissions modeling, vehicle activity analysis, advanced navigation techniques, electric vehicle technology, and advanced sensing and control. He served as the IEEE ITSS President for 2014 and 2015. He is also the IEEE ITSS Vice President of Education. He has been active in the IEEE Intelligent Transportation System Society for many years.